100 A Class Hollow Cathode

IEPC-2015-192／ISTS-2015-b-192

*Presented at Joint Conference of 30th International Symposium on Space Technology and Science
34th International Electric Propulsion Conference and 6th Nano-satellite Symposium,
Hyogo-Kobe, Japan
July 4 – 10, 2015*

Shigeru Yokota[1]
University of Tsukuba, Tsukuba, Ibaraki, 305-8573, Japan

Kohei Kojima[2] and Tatsuya Kimura[2]
Mitsubishi Heavy Industry Ltd., Nagoya, Aich, 485-8561, Japan

and

Hisashi Kataoka[3] and Akihiro Sasoh[4]
Nagoya University, Nagoya, Aich, 464-8603, Japan

Abstract: For recent high power electric propulsion systems in the range of several tens to 100 kW for cargo and manned missions, we have designed and manufactured a 100 A class hollow cathode. As a result of the operation test, we succeed to extract 100 A of electron current. The voltage-current characteristic of the hollow cathode was dependent on the propellant species but independent on the propellant mass flow rate and the orifice diameter. In order to analyze the hollow cathode plasma, a particle simulation code is under development. In this paper, we also report the current status.

Nomenclature

A	=	Richardson constant
D	=	diffusion coefficient
J	=	emission current
j	=	emission current density
k	=	Boltzmann constant
L, R	=	insert length and radius
n_e	=	electron number density
n_n	=	neutral particle number density
r, z	=	components of cylindrical coordinate
T	=	temperature of electron emitter
T_e	=	electron temperature
ϕ	=	work function of electron emitter
Γ	=	flux
σ_i	=	ionization cross section

[1] Associate Proffesor, Department of Engineering Mechanics and Energy, yokota@kz.tsukuba.ac.jp.
[2] Nagoya Guidance and Propulsion Systems Works, kohei_kojima@mhi.co.jp
[3] Graduate Student, Department of Aerospace Engineering
[4] Professor, Department of Aerospace Engineering, sasoh@nuae.nagoya-u.ac.jp.

I. Introduction

RECENTLY, high power electric propulsion systems for deep space exploration or mars mission have been developed.[1] Especially, Hall thrusters and magnetplasmadynamic (MPD) thrusters are hopeful candidates for theses missions because of their high thrust densities. These thrusters require high current hollow cathode. For instance, discharge current of the hall thruster for the mars mission is 100 A.[2] A MPD thruster also need a high current hollow cathode to reduce the cathode erosion problem.[3]

One of the most remarkable research of a high current hollow cathode is conducted in JPL/NASA.[4] They developed a hollow cathode with a LaB_6 insert which can emit 200 A of the electron current for high power Hall thrusters or Ion engines. We have also designed and manufactured a high current hollow cathode with a LaB_6 insert for the above mentioned MPD thruster[3] or other thrusters. Also we develop a particle simulation code in order to obtain the plasma profile in the hollow cathode. In this paper, we report the experimental performance and the numerical simulation result.

II. Hollow cathode design

A. Insert design

According to the Richardson-Dushman equation, electron emission current density from a material is

$$j = AT^2 \exp\left[-\frac{\varphi}{kT}\right], \tag{1}$$

where, A, T, ϕ, and k are Richardson constant, the material temperature, work function and Boltzmann constant, respectively. Only ϕ is the specific value of each materials in this equation. Figure 1 shows the emission current density j as a function of T. Here, ϕ values can be found in reference 5 and 6. Oxidized Barium (BaO) impregnated Tungsten (W) is the lowest work function material, while, BaO is easy to degrade in the Oxygen atmosphere.[7] Therefore, we adopt the LaB_6 as the electron emitter material.

The emission current density of the operation point of a hollow cathode, in general, is about j=10 A/cm^2. Therefore, the operation temperature is set on 1900 K. The total electron emission current J is

$$J = 2\pi RLj \tag{2}$$

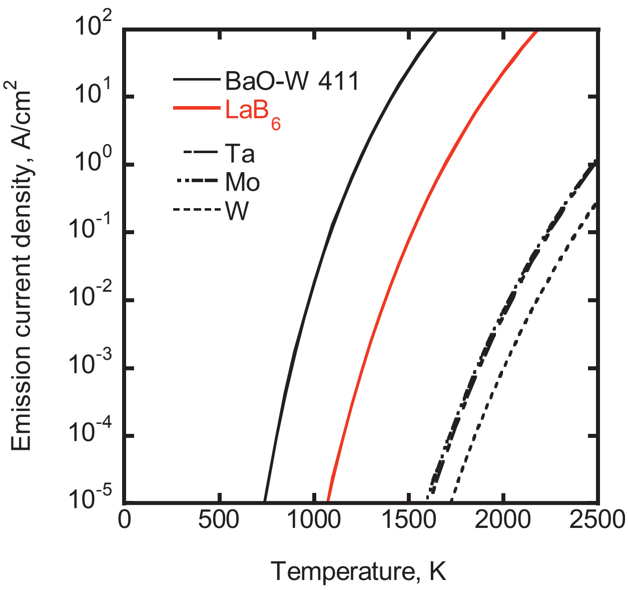

Figure 1. Emission current density as a function of the material temperature.

where, R and L is inner radius and length of the insert, respectively. We set the target value of J is 100 A, so that, the inner surface of the insert can be derived from this equation.

The radius and length are determined by the following plasma modeling.[8] From the steady state electron equation of continuity

$$\nabla\Gamma = \dot{n}_{\mathrm{e}} \tag{2}$$

and diffusion equation

$$\Gamma = -D\nabla n_{\mathrm{e}} \tag{3}$$

we obtain

$$D\nabla^2 n_{\mathrm{e}} = n_{\mathrm{n}} n_{\mathrm{e}} \sigma_{\mathrm{i}} \overline{v_{\mathrm{e}}} \tag{4}$$

where, D, n_n, n_e, σ_i and v_e are diffusion coefficient, neutral number density, electron number density, ionization collision cross section, and electron velocity, respectively. This equation indicates the electron number density depends on the diffusion and ionization. This equation in the cylindrical coordinate can be solved under the boundary condition of $n_e(R, z)$ =0.

$$n_e(r,\ z) = n_e(0,\ 0)\, J_0\left(\frac{\lambda_{01}}{R} r\right) e^{|\alpha| z}\,. \tag{5}$$

Here, J_0 is Bessel function of the first kind, λ_{01}=0.2405 and α is a function of T_e. This solution indicates the plasma density is exponentially decrease toward the upstream; too long L is meaningless for plasma production. From the solution, we define an appropriate L and R.

B. Thermal design

In general, the insert is heated by a heater. A sheath heaters are used in many cases, however we adopt a coil heater insulated from the cathode body and the keeper by ceramic tubes because of its availability. The cathode configuration were determined by fabrication limitation and a simple thermal analysis (Fig. 2). To estimate the heat from the plasma, NASA's analysis model[8] is referred.

C. Structure

Figure 3 shows the schematic of the hollow cathode we designed and fabricated. The insert material is LaB_6 as mentioned above. The cathode body is made of Tantrum because of its high melting point and machinability. The other high temperature components are made of Molybdenum or INCO718. The SUS is used for the components which temperature is not so high. Insulators are made of Almina.

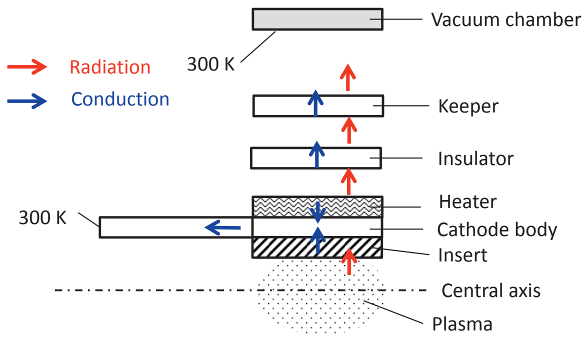

Figure 2. Schematic of the simple thermal analysis.

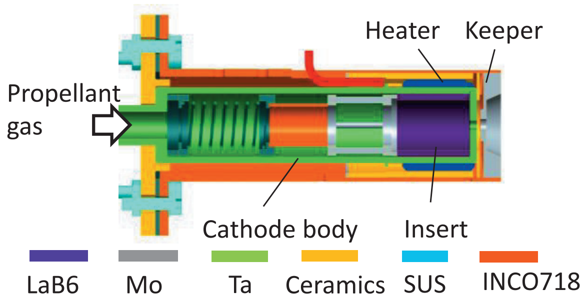

Figure 3. Hollow cathode structure.

III. Operation test

A. Experimental setup

Figure 4 shows the experimental setup. The hollow cathode operated in a vacuum chamber which length and diameter were 3 m and 2 meter, respectively. The chamber is evacuated by a turbo molecular pomp (3200 L/s) backed by a rotary pump (33 L/s) and reached around 1.0×10^{-3} Pa.

The cathode was set in the vacuum chamber. An anode plate was set in 30 mm downstream. All of the cathode components and the anode are insulated from the vacuum chamber. The operation parameter is tabulated on Table 1.

Table 1. Experimental parameters

Parameters	Values
Gas species	Ar, Xe
Propellant flow rate, Aeq.	1, 5
Heater current, A	17 ~ 19
Keeper current, A	1
Anode current, A	40 ~ 100
Cathode orifice diameter, mm	1, 3

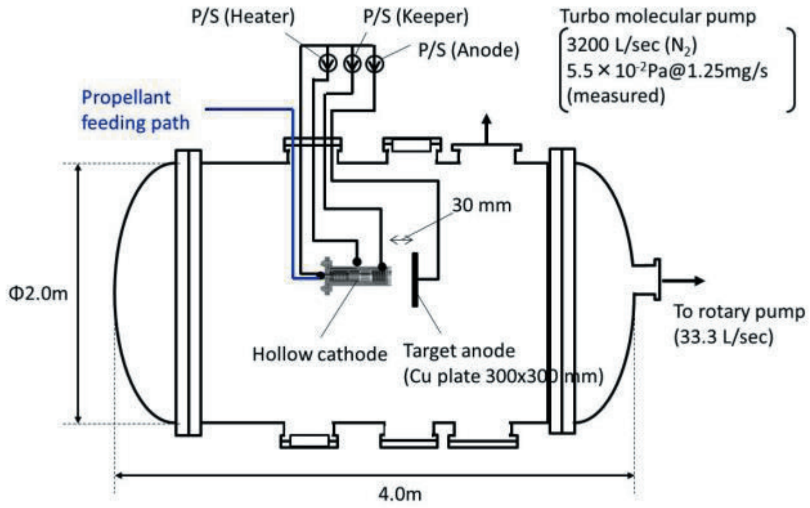

Figure 4. Experimental setup.

B. Result

Figure 5 is a picture of hollow cathode operation. Figure 6 shows a typical discharge current and voltage history. In 100 sec after ignition, the discharge current reached to the target value 100 A. This must be because the insert temperature was gradually increased by the heat from the plasma.

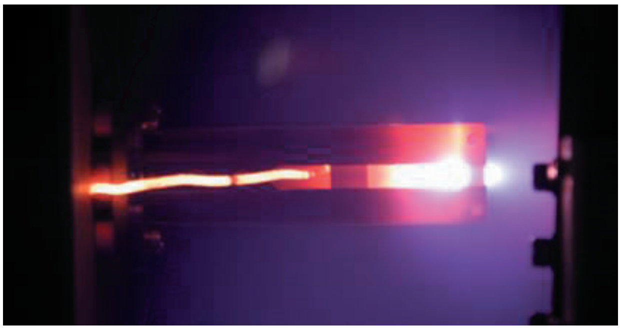

Figure 5. Hollow cathode operation.

Figure 7 shows the voltage-current characteristic of the hollow cathode. The anode voltage decrease with increment of the anode current. This might be because the larger anode current gives the insert more heat from plasma. The V-I characteristic does not so much depends on the propellant mass flow rate and the orifice diameter. When Argon is used as a propellant, the anode voltage is higher than that in the case of Xenon, which is caused by the difference of ionization energies.

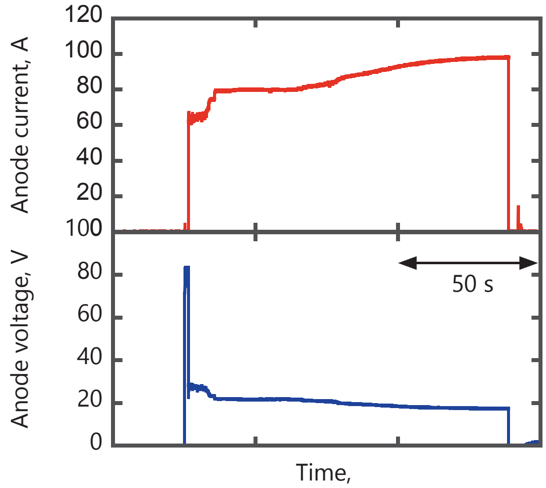

Figure 6. Typical time history of anode current and voltage.

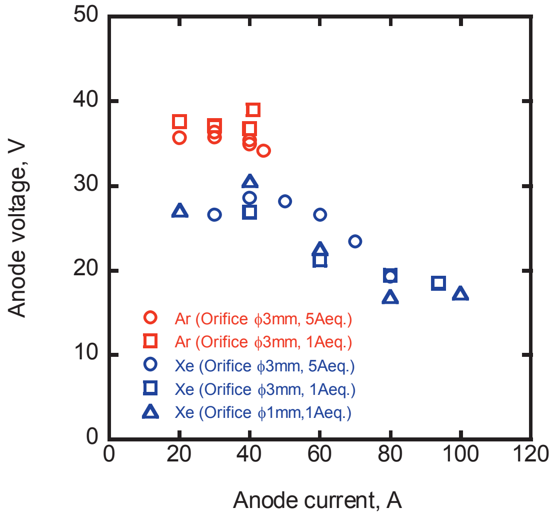

Figure 7. Voltage-current characteristic.

IV. Numerical simulation

A. Methods

The calculation region is from inside the hollow cathode to the anode target (Fig. 8). Since potential drop is expected to be appeared not only on the wall but also in the orifice area, we adopt fully kinetic particle in cell method, which can solve the potential without any assumption, is used. Cylindrical coordinate system is used. Spatial dimension and velocity spatial dimension are two and three, respectively.

Collision is solved by using Direct Simulation Monte Carlo (DSMC). Only three dominant electron – neutral particle collisions, elastic scattering, ionization, and excitation, are considered.

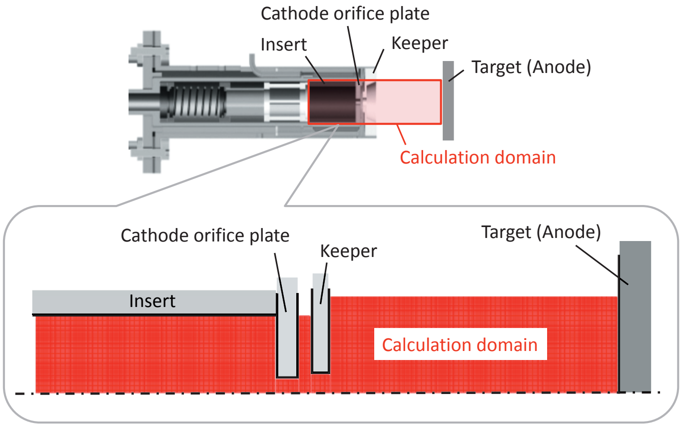

Figure 8. Calculation domain.

The particle equation of motion is solved by Buneman-Boris method. Neutral particles flow through the upstream side boundary. Electrons emit from the insert surface. On the wall, neutral particles scatter randomly with wall temperature energy. Ions recombine and become neutral particle on the wall (Fig.9 (a)).

To obtain the electric field, Poisson's equation was solved by GMRES method. The cathode potential was set at 0 V. The anode potential and the keeper potential are changed by each currents. On the other boundary, Neumann condition was applied (Fig.9 (b)).

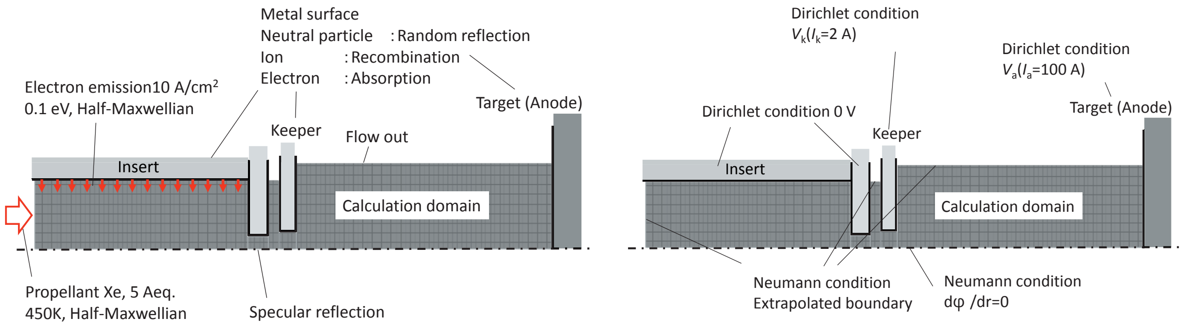

(a) Particle **(b) Electric field**

Figure 9. Boundary conditions.

B. Current status

The calculation is still undergoing; here, we report the current status. A typical cathode current history is shown in Fig. 10. The current was oscillated but the average current was 100 A. The oscillation seems to be a noise of particle simulation. The currents of each parts are tabulated on Table 2. When the emission current from the insert was set at 40 A, the ion and electron current from the plasma to the insert was shown by the table. As a result, the average cathode current was about 100 A. On the other hand, the anode current was only 40 A, so that a part of the electron emitted from the cathode does not absorbed by the anode.

Figure 11 shows the electron number density distribution. As shown in this figure, the electron number density takes maximum on the central axis, which is qualitatively similar to the electron number density distribution predicted by the theoretical plasma model (Eq. (5)). More precise analysis using the numerical simulation code is our future work.

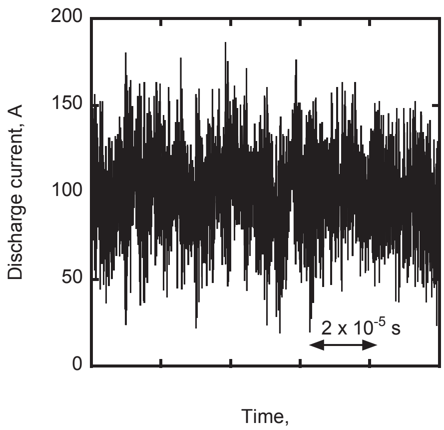

Figure 10. Cathode current history

Table 2. Breakdown of currents

Cathode current, A	(total)	9.98×10^{1}
	(emission)	4.00×10^{1}
	(electron)	2.53×10^{4}
	(ion)	2.53×10^{4}
Anode current, A	(total)	3.57×10^{1}
	(electron)	3.67×10^{1}
	(ion)	1.00×10^{0}
Keeper current, A	(total)	-3.89×10^{0}
	(electron)	2.42×10^{2}
	(ion)	2.46×10^{2}

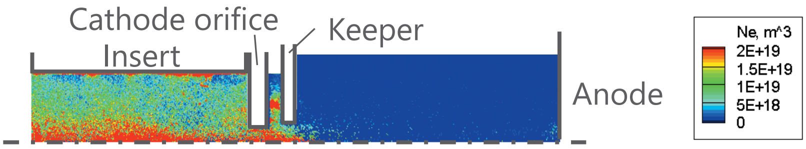

Figure 11. Electron number density distribution.

V. Conclusion

We have designed and manufactured a 100 A class hollow cathode. As a result of the operation test, we succeed to extract 100 A of electron current. The voltage-current characteristic of the hollow cathode was dependent on the propellant species but independent on the propellant mass flow rate and the orifice diameter. In order to analyze the hollow cathode plasma, a particle simulation code is under development. The simulation was semi-converged. The more precise analysis is our future work.

Acknowledgments

This research was partially supported by the Ministry of Education, Science, Sports and Culture, Grant-in Aid for Young Scientists (A), 2015-2018（15H05558）.

References

[1]website: http://www.globalspaceexploration.org/wordpress/

[2]N. Yamamoto, K. Takase, Y. Hirano, K. Komurasaki, A. Kakakmi, R. Tsukisaki, S. Hosoda, H. Kuninaka, and S. Yokota, "Thrust performance in 5 kW class anode layer type Hall thruster," IEPC-Paper-2015-459p.

[3]D. Ichihara, S. harada, H. Kataoka, S. Yokota, and A. Sasoh, "Operation Characteristics of Steady-State, Applied Field, Rectangular Magnetoplasmadynamics (MPD) Thruster, Journal of the Japan Society for Aeronautical and Space Sciences, Vol.63, No.2, pp.37-44, 2015. (in Japanese)

[4] Goebel, D. M. and Chu, E., "High-Current Lanthanum Hexaboride Hollow Cathode for High-Power Hall Thrusters," Journal of Propulsion and Power, Vol.30, No.1, pp.35-40, 2014.

[5] J. L. Cronin, "Modern Dispenser Cathodes," IEE Proceedings, vol.128, no.19, 1981.

[6] W. H. Kohl, "Handbook of Materials and Techniques for Vacuum Devices," American Institute of Physics, 1995.

[7] J. L. Cronin, "Practical Aspects of Modern Dispenser Cathodes," Microwave Journal, vol. 22, pp.57-62, 1979.

[8] D. Goebel, I. Katz, "Fundamental of Electric Propulsion, Wiley, pp.243-324, 2008.